communications biology

A Nature Portfolio journal

Article

https://doi.org/10.1038/s42003-025-07856-9

The influence of *Lactobacillus johnsonii* on tumor growth and lymph node metastasis in papillary thyroid carcinoma

Minghao Xie[1], Tingting Yang[2], Qiang Liu[1], Zhikun Ning[3], Lili Feng[4,5,6] ✉ & Xiang Min[2,6] ✉

Lymph node metastasis (LNM) is a key factor in the prognosis of papillary thyroid carcinoma (PTC). This study explores the effect of intratumoral bacteria on LNM in PTC. The intrathyroidal microbiome is analyzed in 55 PTC patients by 16S rRNA gene sequencing. The CCK8 and Transwell assays determine the impact of bacteria on the proliferation and migration abilities of PTC cells. Xenograft tumor and bacterial colonization experiments are carried out using nude mice. We show that *Lactobacillus* is significantly decreased in PTC lesions from patients with LNM. *Lactobacillus johnsonii* (*L. johnsonii*) suppresses the proliferation and migration capability of PTC cells in vitro and in vivo. Bacterial gut colonization of *L. johnsonii* increases its abundance in tumors and inhibits PTC growth and LNM. These findings suggest that *L. johnsonii* can be harnessed for the development of innovative therapeutic strategies for PTC.

Thyroid cancer is the most common endocrine malignancy worldwide, of which papillary thyroid cancer (PTC) is the most common subtype[1]. The increasing incidence of PTC is mainly due to the more frequent use of neck ultrasonography and fine-needle aspiration of thyroid nodules[2]. In spite of the favorable prognosis of PTC, it is reported that over half of patients develop cervical lymph nodes metastasis (LNM) which is a major risk factor for disease recurrence[3,4]. Thus, controlling the LNM of PTC may be an effective measure to further improve the prognosis of patients.

Recent researches have indicated that microbiota, particularly the gut microbiota, is involved in the initiation, progression and dissemination of cancer[5]. Gut microbiota potentially influence individual's susceptibility to cancer, and certain bacteria have been reported to accelerate tumor growth and metastatic progression[6,7]. Besides, microbiota has ability to modify the microenvironment within tumor and could thereby enhance tumor response to therapeutic drugs. Previous research demonstrated that fecal microbiota transplantation from responders significantly improved tumor-suppressing efficacy of PD-1 blockade, suggesting the potential contribution of the microbiota in tumor treatment[8]. Specifically, alterations of intestinal microbial community have also been found to correlate with pathogenesis and therapy response of thyroid carcinoma[9,10]. Yet, considering the thyroid's anatomical separation from intestine, the precise association and underlying mechanism between thyroid cancer and bacteria remains uncertain.

The relationship between tumor cell with intratumoral bacteria and the initiation, growth, metastasis, and resistance to chemotherapy of tumors is widely acknowledged[11]. A study conducted on PTC patients revealed notable variations in the intratumoral microbiome characteristics based on patients' age and tumor stage[12]. Another study has identified significant differences in microbial diversity and composition between the peritumor and tumor microhabitats of patients with thyroid cancer, with a potential correlation between a higher abundance of *Sphingomonas* and LNM[13]. However, there is a scarcity of research examining the involvement of intratumoral bacteria in thyroid cancer. The aforementioned studies solely relied on the analysis of 16S rRNA gene sequencing data and did not conduct experimental investigations to validate their hypotheses.

In this study, we successfully isolated and cultured intrathyroidal bacteria under both anaerobic and aerobic conditions. Additionally, we established a nude mice LNM model of PTC by subcutaneously injecting a fluorescently labeled PTC cell line. Our findings reveal that intratumoral *Lactobacillus johnsonii* (*L. johnsonii*) is more prevalent in non-metastatic PTC, and it exerts inhibitory effects on LNM by suppressing the epithelial-mesenchymal transition (EMT) process. Significantly, we demonstrated that the oral administration of *L. johnsonii* can enhance its colonization in the gut and intratumoral regions, suggesting its potential as a novel therapeutic approach to inhibit LNM in PTC.

[1]Department of General Surgery, the First Affiliated Hospital, Jiangxi Medical College, Nanchang University, Nanchang, Jiangxi, 330006, PR China. [2]Department of Otolaryngology, Head and Neck Surgery, the First Affiliated Hospital, Jiangxi Medical College, Nanchang University, Nanchang, Jiangxi, 330006, PR China. [3]Department of Day Ward, the First Affiliated Hospital, Jiangxi Medical College, Nanchang University, Nanchang, Jiangxi, 330006, PR China. [4]State Key Laboratory of Oncology in South China, Collaborative Innovation Center for Cancer Medicine, Sun Yat-sen University Cancer Center, Guangzhou, Guangdong, 510000, PR China. [5]Department of Radiology, Sun Yat-sen University Cancer Center, Guangzhou, Guangdong, 510000, PR China. [6]These authors jointly supervised this work: Lili Feng, Xiang Min. ✉e-mail: fengll2@sysucc.org.cn; ndyfy01295@ncu.edu.cn

Results

Intratumoral *Lactobacillus* was enriched in Non-metastatic PTC

To investigate the impact of intrathyroidal microbiomes on LNM of PTC, we collected tumor tissues and adjacent non-tumor (normal) tissues from 55 PTC patients and performed 16S rRNA gene sequencing. The demographic and clinical characteristics of patients with PTC were shown in Table 1. There was no significant difference in community composition at phylum level between tumor and normal tissue, of which the three predominant bacteria were *Proteobacteria*, *Actinobacteriota*, and *Firmicutes*. (Fig. 1a, b). Subsequent LEfSe analysis at genus level revealed a significant enrichment of *Cutibacterium* and *Gaiella* in the normal tissues, while *Herbaspirillum* and *Coprococcus* were enriched in tumor tissues (Fig. 1c, d). Moreover, we divided the tumor tissues into two groups by LNM and found that the abundance of *Lactobacillus* was the most significant difference between the metastasis group ($n = 29$) and non-metastasis group ($n = 26$) (Fig. 1e, f).

Lactobacillus johnsonii was presented in PTC tissues

To confirm the presence of bacteria in the thyroid, we utilized high-resolution electron microscopy (EM) analysis, which revealed the presence of bacteria in both tumor and adjacent normal tissues (Fig. 2a). Subsequently, we collected tumor and adjacent normal tissues from 8 additional PTC patients, and the intrathyroidal bacteria isolated from these tissues were cultured under anaerobic and aerobic conditions. As shown in Fig. 2b, colonized bacteria were found in thyroid tissues of 3 patients both under anaerobic and aerobic conditions. Specifically, in Patient Nos. 60 and 62, bacteria could be found both in tumor and normal tissues, while in Patient No. 63, bacteria could be found only in tumor tissue. To identify the specific bacteria strain in these 3 patients, we picked the single colony and ran colony PCR to get the bacteria sequencing. By aligning to the 16S rRNA sequences database in the NCBI BLAST site, we found out that the main bacteria strain was *Escherichia coli* (*E. coli*) in Patient No. 60 and No. 63 both under anaerobic and aerobic conditions. Comparatively, *Lactobacillus johnsonii* (*L. johnsonii*) was mostly presented in the tumor tissue of Patient No.62 under anaerobic condition (Fig. 2b). Additionally, the 16S sequencing data revealed that *L. johnsonii* represented the highest proportion of *Lactobacillus* at the species level in 55 PTC patients (34%) (Supplementary Fig. 1a). We further confirmed the presence of *L. johnsonii* in both tumor and normal tissues through Fluorescence in situ hybridization (FISH) (Fig. 2c). The quantitative statistical analysis of *L. johnsonii* expression in the 16S-FISH assay revealed that its abundance in normal tissues was significantly higher than in tumor tissues (Fig. 2d).

Lactobacillus johnsonii suppressed proliferation, invasion and migration of human PTC cells via inhibiting Wnt/β-catenin pathway

To investigate the roles of *Lactobacillus* in PTC, we examined the correlation between tumor volume and the abundance of *Lactobacillus* in 55 PTC patients. The 55 PTC patients were divided into two groups according to the median abundance value of *Lactobacillus*. As shown in Fig. 3a, the group with low abundance of *Lactobacillus* exhibited larger tumor sizes than the other group with high abundance of *Lactobacillus*. The correlation analysis showed that there was a significant negative correlation between the abundance of *Lactobacillus* and tumor volume. The representative sequence of each ASV belonging to *Lactobacillus* was further aligned to the NCBI 16S BLAST database to identify the ASV of *L. johnsonii*. As shown in Fig. 3b, the abundance of *L. johnsonii* was significantly lower in tumor tissues compared to normal tissues. Consequently, the 55 PTC patients were divided into another two groups according to the median abundance value of *L. johnsonii*. Similarly, group with low abundance of *L. johnsonii* also exhibited larger tumor sizes than that with high abundance of *L. johnsonii*. (Fig. 3c), indicating a significant negative correlation between the abundance of *L. johnsonii* and tumor volume (Fig. 3d). We evaluated cell proliferation of IHH4 and TPC1 cells treated with different MOI of *L. johnsonii*. As shown in Fig. 3e, f, the higher MOI of *L. johnsonii* initially introduced, the more slowly the IHH4 and TPC1 cells proliferated.

According to the findings depicted in Fig. 3g, h, there was a significant reduction in the relative abundances of *Lactobacillus* and *L. johnsonii* in tumor tissues with LNM compared to those without LNM. To investigate the potential impact of *L. johnsonii* on the invasion and migration of PTC cells, a Transwell invasion and migration assay was conducted using IHH4 and TPC1 cells co-cultured with *L. johnsonii*. As shown in Fig. 3i, j, L. *johnsonii* significantly inhibited the invasion and migration ability of IHH4 and TPC1 cells compared with cells co-cultured with *E. coli* (isolated from PTC) or 1×PBS as negative controls.

Previous study suggested that *L. johnsonii* could regulate the β-catenin pathway to inhibit the metastasis of colorectal cancer. We wondered whether β-catenin signaling pathway was involved in *L. johnsonii* suppressing PTC growth and metastasis, and detected the related proteins. The results showed that β-catenin, c-MYC, N-cadherin and Vimentin was down-regulated, accompanied with markedly up-regulated E-cadherin in IHH4 and TPC1 cells after co-cultured with *L. johnsonii* (Fig. 4a). Following the inhibition of β-catenin expression in IHH4 and TPC1 cells using shRNA (Fig. 4b), the inhibitory effects of *L. johnsonii* on tumor cell growth, migration, and invasion were markedly reduced (Fig. 4c–f). These results indicate that *L. johnsonii* exerts its antitumor effects primarily by suppressing the β-catenin signaling pathway.

L. johnsonii suppressed tumor growth and LNM of PTC in vivo

A xenograft tumor experiment in nude mice was conducted to verify the potential effect of *L. johnsonii* on PTC. As shown in Fig. 5a, the IHH4-Luciferase cell line labeled with nano carbon tracer was used to observe tumor formation and metastasis. As described in the "METHODS" section, the mouse LNM model of PTC was established by *L. johnsonii*, *E. coli* or PBS pretreated IHH4-Luciferase cells subcutaneously injection and the subcutaneous tumors were excised on day 28 (Fig. 5b). In the *L. johnsonii* treated group, the size and weight of xenograft tumor were significantly lower compared with the *E. coli* and PBS treated groups (Fig. 5c, d). Furthermore, after removal of subcutaneous tumor, the *L. johnsonii* treated group showed a significantly lower LNM rate compared with the *E. coli* and PBS treated groups (Fig. 5e, f). These results indicated that the *L. johnsonii* was capable of suppressing tumor growth and metastasis of PTC in vivo.

Gut colonization of *L. johnsonii* inhibited PTC metastatic progression

Considering that the main colonization site of *L. johnsonii* was gastrointestinal tract and the oral intake was the main way that human get *L. johnsonii*, we collected fecal tissues from those 55 PTC patients and performed qPCR to detect the abundance of *L. johnsonii*. The qPCR results indicated that the abundance of *L. johnsonii* in the feces of metastatic group was significantly lower than that of non-metastatic group (Fig. 6a). The correlation analysis revealed a significant positive correlation between the abundance of *L. johnsonii* in patients' tumors and their feces (Fig. 6b). Then we performed gut colonization mice experiment to investigate the impact of *L. johnsonii* on LNM of PTC. Mice implanted with subcutaneous IHH4-Luciferase cell lines were gavaged with MRS, *E. coli*, or *L. johnsonii* after 5-day treatment of antibiotic cocktails (Fig. 6c). Indeed, the xenograft tumor volume and weight (Fig. 6d) were significantly lower in *L. johnsonii* gavaged group compared with the *E. coli* and MRS gavaged groups, supporting that *L. johnsonii* significantly inhibited tumor growth of PTC in vivo.

To certify that the tumor suppression was modulated by gut colonization of *L. johnsonii*, mice fecal and xenograft tumors were collected after 28 days of colonization gavage. Compared with the *E. coli* and MRS gavaged groups, the abundance of *L. johnsonii* in mice fecal was significantly increased in *L. johnsonii* gavaged group (Fig. 6e), and similar results were observed in xenograft tumors (Fig. 6f). Moreover, the LNM of PTC was evaluated by in vivo bioluminescence imaging system, and the fluorescence was significantly decreased in the *L. johnsonii* gavaged group compared with the *E. coli* and MRS gavaged groups (Fig. 6g). The above results suggested

Table 1 | The demographic and clinical characteristics of the PTC patients

Patient ID	Sex	Age (year)	TNM stage	Clinical stage	Extrathyroid extension	Vascular invasion	LNM	Concomitant HT
1	Female	29	T1aN1aM0	1	No	No	Yes	No
2	Female	35	T1aN0M0	1	No	No	No	No
3	Female	49	T1aN1aM0	1	Yes	No	Yes	No
4	Female	41	T1aN0M0	1	Yes	No	No	No
5	Female	41	T4aN1bM0	1	Yes	No	Yes	Yes
6	Female	66	T1bN0M0	1	No	No	No	No
7	Male	35	T1bN1aM0	1	No	No	Yes	No
8	Female	34	T1aN0M0	1	No	No	No	No
9	Female	56	T1bN0M0	1	No	No	No	No
10	Female	41	T1aN0M0	1	No	No	No	Yes
11	Female	65	T1aN0M0	1	No	No	No	No
12	Male	38	T1aN1bM0	1	No	No	Yes	No
13	Female	34	T1bN0M0	1	Yes	No	No	Yes
14	Female	38	T1aN0M0	1	No	No	No	No
15	Female	37	T1bN0M0	1	No	No	No	No
16	Female	55	T1aN1aM0	2	No	No	Yes	No
17	Female	34	T1bN1bM0	1	No	No	Yes	Yes
18	Female	33	T1bN1bM0	1	No	No	Yes	No
19	Female	67	T4aN1bM0	3	Yes	Yes	Yes	Yes
20	Female	17	T2N1bM0	1	Yes	Yes	Yes	No
21	Male	38	T2N1bM0	1	Yes	Yes	Yes	No
22	Male	52	T4aN0M0	1	Yes	Yes	No	No
23	Female	53	T1bN0M0	1	No	No	No	No
24	Female	49	T4aN1bM0	1	Yes	No	Yes	Yes
25	Male	59	T4aN1bM0	3	Yes	No	Yes	Yes
26	Male	49	T1bN1aM0	1	No	No	Yes	No
27	Female	56	T1bN1aM0	2	No	No	Yes	Yes
28	Female	56	T3bN0M0	1	Yes	No	No	No
29	Female	49	T1aN0M0	1	No	No	No	No
30	Female	47	T2N1aM0	1	No	No	Yes	Yes
31	Female	21	T2N1bM0	1	Yes	Yes	Yes	Yes
32	Female	70	T1aN1aM0	2	No	No	Yes	Yes
33	Female	52	T1aN1aM0	1	No	No	Yes	No
34	Female	40	T1aN0M0	1	No	No	No	No
35	Female	60	T3bN0M0	1	Yes	No	No	Yes
36	Female	42	T1aN1aM0	1	Yes	Yes	Yes	Yes
37	Female	25	T2N1bM0	1	No	No	Yes	No
38	Female	34	T1bN0M0	1	No	No	No	No
39	Female	41	T1bN0M0	1	No	No	No	No
40	Female	54	T1aN0M0	1	No	No	No	Yes
41	Female	55	T4aN1bM0	3	Yes	Yes	Yes	No
42	Male	66	T4aN1aM0	3	Yes	No	Yes	Yes
43	Male	29	T1bN0M0	1	No	No	No	Yes
44	Male	60	T1bN1aM0	2	No	No	Yes	No
45	Female	31	T2N1bM0	1	No	No	Yes	Yes
46	Female	52	T1aN0M0	1	No	No	No	No
47	Female	33	T1aN0M0	1	No	No	No	No
48	Female	52	T1aN0M0	1	No	No	No	No
49	Female	45	T1bN0M0	1	No	No	No	No
50	Male	49	T4aN1aM0	1	Yes	Yes	Yes	No
51	Male	48	T1bN0M0	1	No	No	No	No

Table 1 (continued) | The demographic and clinical characteristics of the PTC patients

Patient ID	Sex	Age (year)	TNM stage	Clinical stage	Extrathyroid extension	Vascular invasion	LNM	Concomitant HT
52	Male	33	T1aN0M0	1	No	No	No	No
53	Female	43	T1bN1aM0	1	No	No	Yes	Yes
54	Female	39	T1bN1aM0	1	No	No	Yes	No
55	Female	56	T2N1aM0	2	Yes	Yes	Yes	Yes

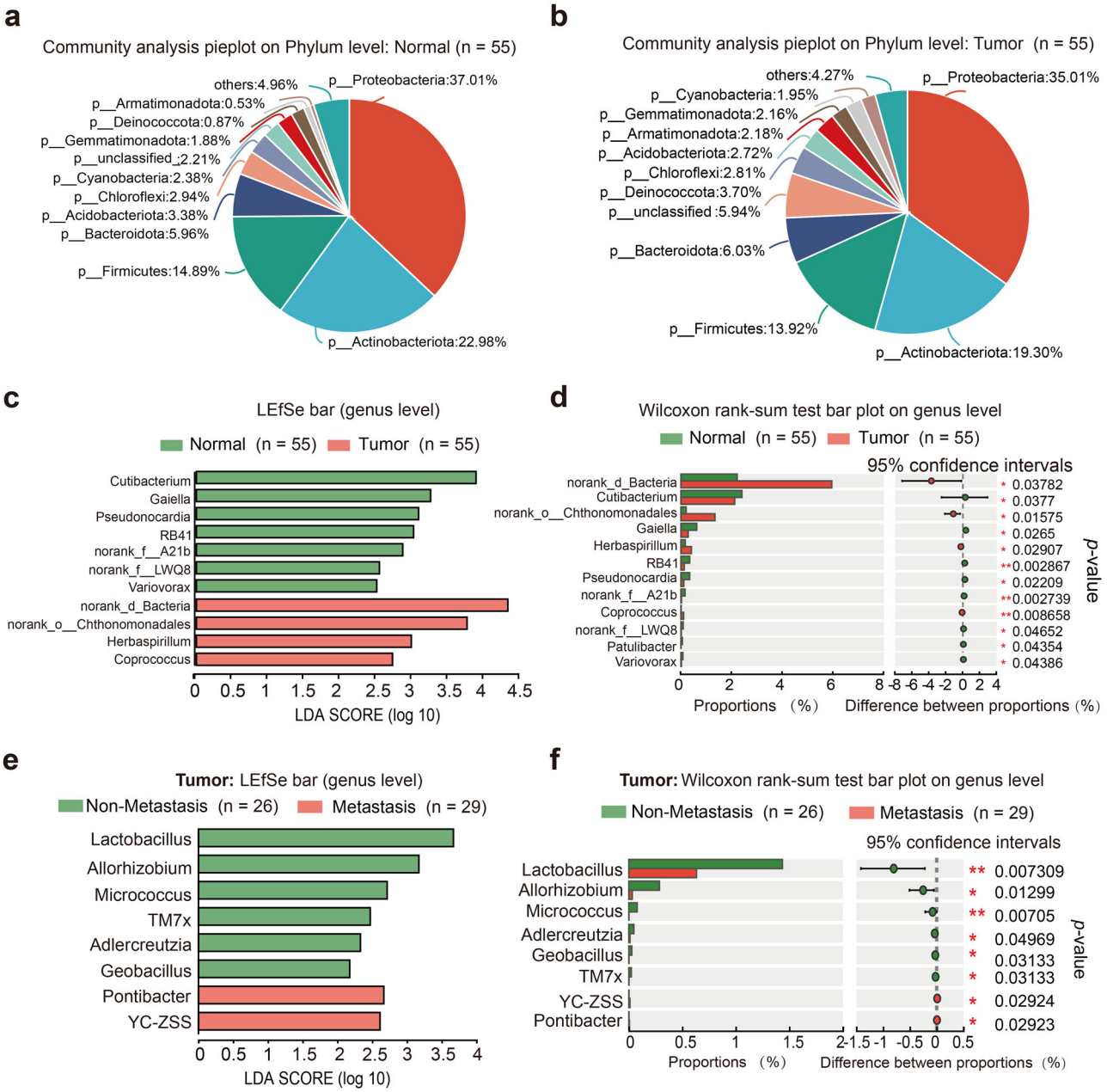

Fig. 1 | Intratumoral *Lactobacillus* was enriched in Non-metastatic PTC. **a** Community analysis pieplot of adjacent normal tissues at phylum level. **b** Community analysis pieplot of tumor tissues on phylum level. **c**, **d** Differential distributed taxa by LEfSe between normal and tumor tissues at genus level. **e**, **f** Differential distributed taxa by LEfSe in tumors between metastasis group and non-metastasis group at genus level.

that *L. johnsonii* was able to colonize in the gastrointestinal tract and translocate to PTC tissue to further suppress the proliferation and metastasis of PTC cell. To disclose the mechanism underlying this phenomenon, expressions of β-catenin pathway-related proteins in xenograft tumors were examined by Western blot. Consistently, β-catenin, c-MYC, N-cadherin and Vimentin were downregulated accompanied with marked upregulation of E-cadherin in xenograft tumors of *L. johnsonii* gavaged group compared with the MRS gavaged group (Fig. 6h).

Discussion

Several studies have shown the correlation between gut microbiota and thyroid disease. One study demonstrated that untreated primary

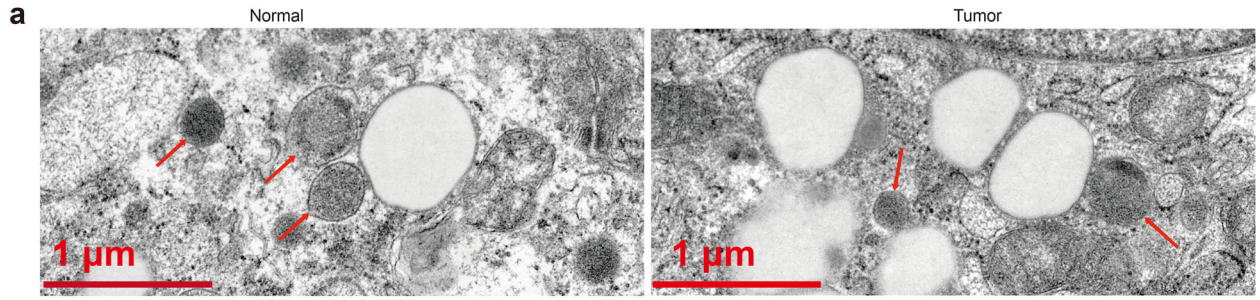

b

	Aerobic (BHI)		Anaerobic (CBA)	
	Normal	Tumor	Normal	Tumor
Patient 59				
Patient 60				
Patient 61				
Patient 62				
Patient 63				
Patient 64				
Patient 65				
Patient 66				
Negative control				

Patient No.	Culture Condition	Location	Bacteria strain
Patient 60	Aerobic	Normal	Escherichia coli
		Tumor	Escherichia coli
			Escherichia fergusonii
	Anaerobic	Normal	Escherichia coli
			Escherichia fergusonii
		Tumor	Escherichia coli
			Escherichia fergusonii
			Bifidobacterium bifidum
			Streptococcus intermedius
			Bacterium NLAE-zl-P143
			Eubacterium sp. strain
Patient 62	Aerobic	Normal	Shigella sonnei
			Cronobacter sakazakii
			Escherichia coli
			Enterococcus thailandicus
		Tumor	Morganella morganii
			Shigella sonnei
			Cronobacter sakazakii
			Enterococcus faecium
			Enterococcus thailandicus
			Escherichia coli
			Microbacterium commune
			Shigella dysenteriae
			Bacteroides fragilis
	Anaerobic	Normal	Shigella sonnei
			Escherichia coli
			Enterococcus thailandicus
			Enterococcus faecium
			Bifidobacterium bifidum
		Tumor	Lactobacillus johnsonii
			Enterococcus thailandicus
			Bifidobacterium bifidum
			Streptococcus salivarius
			Dialister pneumosintes
			Escherichia coli
			Streptococcus intermedius
			Escherichia fergusonii
Patient 63	Aerobic	Normal	Escherichia coli
			Enterococcus durans
	Anaerobic	Tumor	Enterococcus faecium
			Escherichia coli
			Enterococcus durans
			Streptococcus salivarius
			Shigella

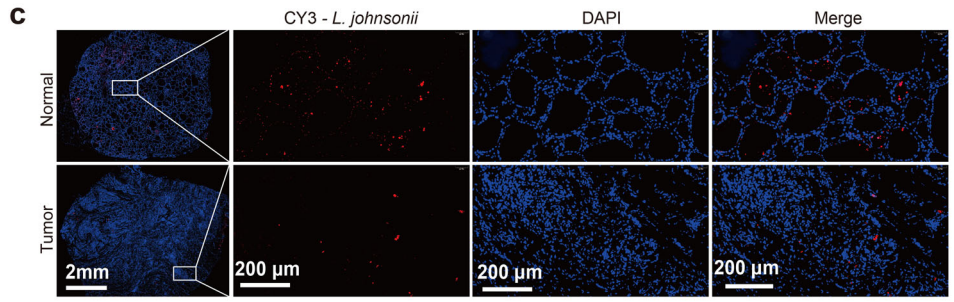

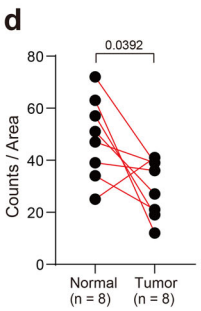

Fig. 2 | *L. johnsonii* was presented in PTC tissues. a EM image of tumor and adjacent normal tissues showing bacteria structures. Red arrows pointing to bacterial structures. Scale bars represent 1 μm. **b** The bacteria colonized from tumor and normal tissues of 8 additional patients were cultured under both anaerobic and aerobic conditions. Identification of the particular strains of bacteria in Patient Nos. 60, 62, and 63 through the utilization of colony PCR and the alignment of 16S rRNA sequences with the NCBI 16S BLAST database available at http://www.ncbi.nlm.nih.gov/BLAST. **c**, **d** Detection of *L. johnsonii* in the CRC tissues from patients by FISH. $n = 8$ biologically independent samples for each group. Scale bars represent 2 mm or 200 μm as labeled.

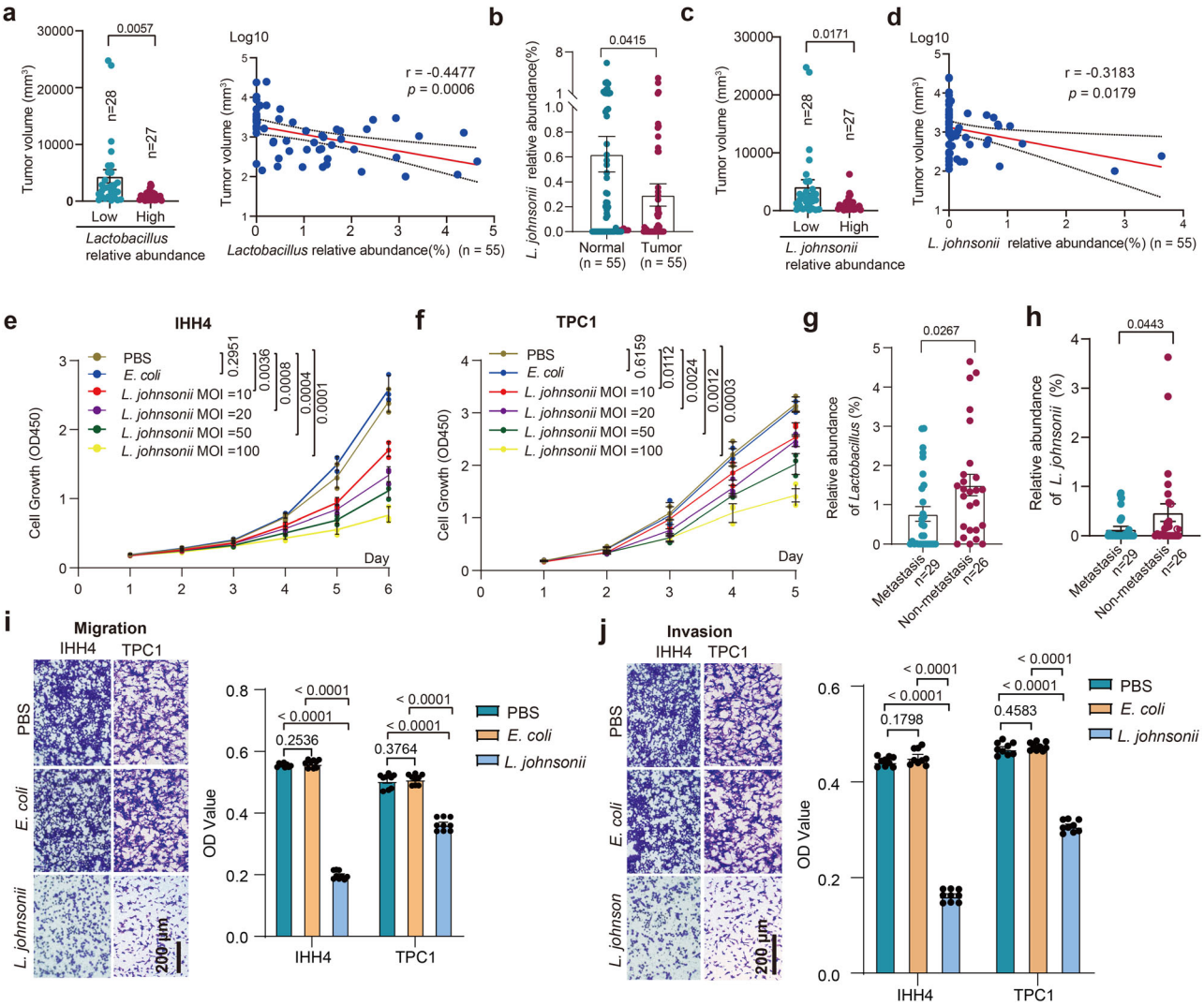

Fig. 3 | *L. johnsonii* suppressed proliferation, invasion and migration of human PTC cells. a Tumor volumes of PTC patients with high or low abundance of *Lactobacillus*, and the correlation analysis between the abundance of *Lactobacillus* and tumor volume. **b** The abundance of *L. johnsonii* in tumor and normal tissues. **c** Tumor volumes of PTC patients with high or low abundance of *L. johnsonii*. **d** The correlation analysis between the abundance of *L. johnsonii* and tumor volume. **e**, **f** CCK8 cell proliferation curve for IHH4 (**e**) and TPC1 (**f**) cells stimulated with indicated MOI of *L. johnsonii*. **g**, **h** Relative abundance of *Lactobacillus* (**g**) and *L. johnsonii* (**h**) in tumor tissues between PTC patients with or without LNM. **i**, **j** Transwell assay evaluated the migration (**i**) and invasion (**j**) abilities of IHH4 and TPC1 cells stimulated with *L. johnsonii*. Error bars indicate standard error of the mean. Scale bars represent 200 μm.

hypothyroidism patients can be differentiated from healthy individuals based on the presence of four specific intestinal bacteria (*Veillonella*, *Paraprevotella*, *Neisseria*, and *Rheinheimera*)[14]. Another study revealed that individuals with hyperthyroidism exhibit reduced levels of *Bifidobacteria* and *Lactobacillaceae*[15]. A separate study found a notable increase in *Bacteroides* and a significant decrease in *Bifidobacterium*, while patients not receiving thyroid hormone replacement therapy displayed higher levels of *Lactobacillus* species compared to those taking oral levothyroxine[16]. In recent years, there has been an expansion of research on the human microbiome, extending beyond the gut, which is known for its abundance of microorganisms, to previously presumed sterile organs such as the bladder and lungs[17,18]. In our study, we utilized 16S rRNA gene sequencing and provided preliminary evidence for the presence of bacteria in the thyroid and PTC. To further validate this discovery, we cultured intrathyroidal bacteria isolated from tumor and normal tissues of an additional 8 PTC patients under both anaerobic and aerobic conditions. Recent evidence suggested that intratumoral bacteria were primarily derived from the digestive tract[19]. Our result showed that a comparable abundance of *L. johnsonii* was observed in the subcutaneous PTC tumor gavage with *L. johnsonii*, suggesting that the intestinal microorganism might translocate to extraintestinal tumor tissue. Bender et al. also reported that probiotic *Lactobacillus reuteri* translocated to, colonized, and persisted within melanoma[20]. However, the possibility of direct bacterial infection at the tumor site via blood vessels could not be completely dismissed.

Multiple studies have provided evidence indicating that intratumoral bacteria possess diagnostic significance for various forms of cancer and show intricate correlation with patient prognosis[21,22]. Extensive researches have elucidated the influence of intratumoral microbiome composition on patient outcomes[23], responses to cancer therapies[24], and the promotion of cancer metastasis[25]. Within the realm of genitourinary cancers, investigators have reported a noteworthy decrease in the abundance of *Lactobacillus* within prostate cancer tissues compared to normal prostate tissues[26]. Furthermore, previous research has demonstrated a correlation between the scarcity of *Lactobacillus* in the lower female reproductive tract and the development of cervical cancer[27]. These findings suggested that *Lactobacillus* might function as a bacterium that suppressed tumor progression. However, Fu et al. reported an enrichment of *Lactobacillus* in breast cancer cells, which were found to inhibit the RhoA-ROCK signaling pathway and induce cytoskeletal remodeling[25]. This mechanism enables tumor cells to withstand mechanical stress within blood vessels, thereby facilitating tumor

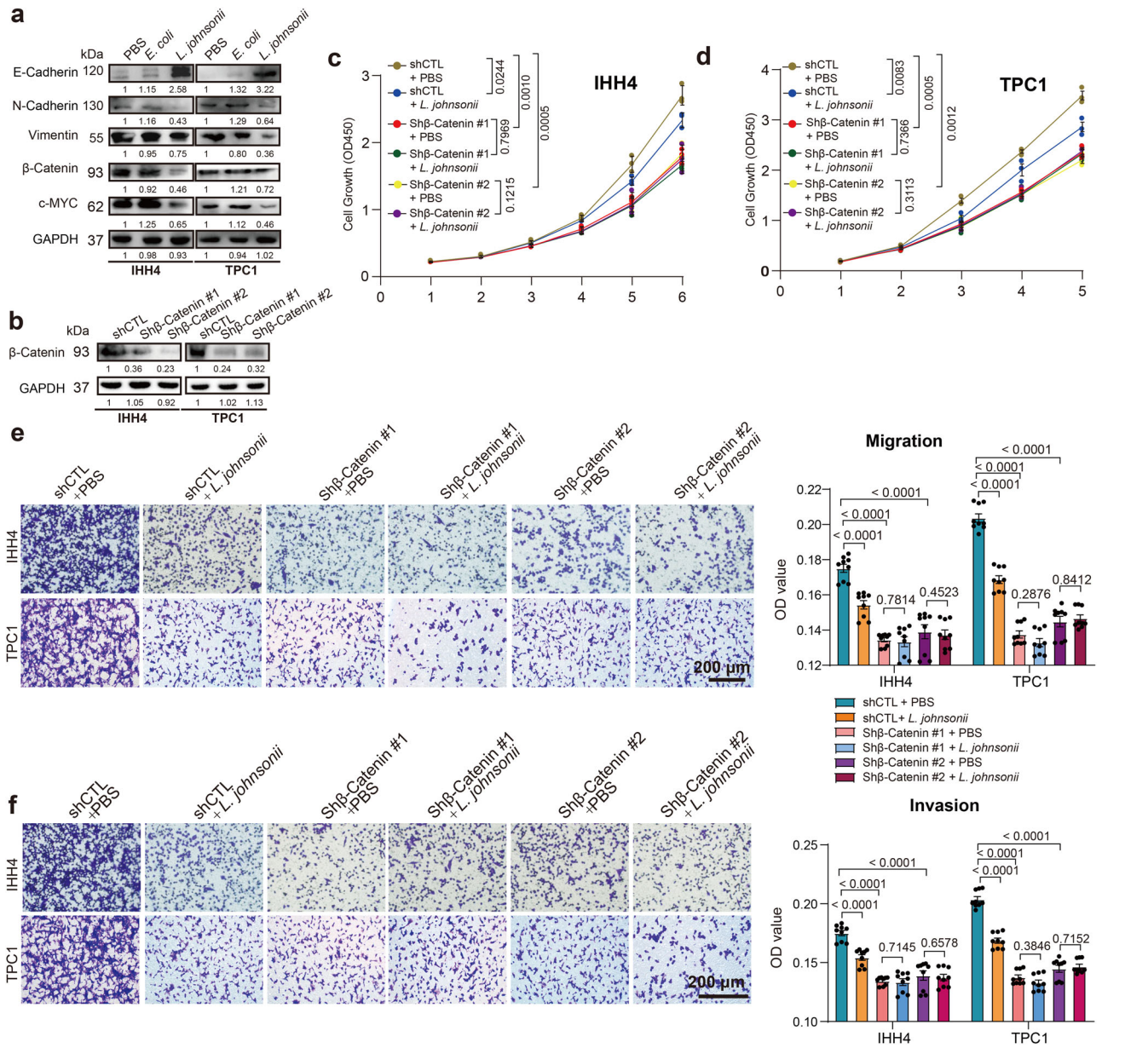

Fig. 4 | *L. johnsonii* suppressed proliferation, invasion and migration of human PTC cells via inhibiting Wnt/β-catenin pathway. a Western blot analysis of Wnt/β-catenin pathway in IHH4 and TPC1 cells after co-cultured with *L. johnsonii*. **b** β-catenin protein expression in IHH4 and TPC1 cell following transfection with shCTL, shβ-catenin #1 or shβ-catenin #2, as determined by Western blot. **c**, **d** CCK8 cell proliferation curves for IHH4 (**c**) and TPC1 (**d**) cells transfected with shCTL, shβ-catenin #1, or shβ-catenin #2 following exposure to *L. johnsonii* or PBS in vitro. **e**, **f** Migration (**e**) and invasion (**f**) assays of IHH4 and TPC1 cells transfected with shCTL, shβ-catenin #1, or shβ-catenin #2 following exposure to *L. johnsonii* or PBS in vitro. Error bars indicate standard error of the mean. Scale bars represent 200 μm.

metastasis. Moreover, through experimentation with germ-free and immunodeficient mice, it has been demonstrated that intracellular bacteria within tumors can promote metastasis autonomously, independent of the intestinal flora and immune system[25]. In our study, analysis of the 16S rRNA gene sequencing data revealed no notable disparities in community composition at the phylum level between tumor and normal tissue of PTC patients. However, a more detailed examination revealed a significant reduction in the abundance of *Lactobacillus* in tumors with LNM compared to tumors without LNM. These results suggested that *Lactobacillus* may play a role in inhibiting the LNM of PTC, thereby acting as a tumor suppressor in this context.

Until now, the effect of intratumoral bacteria on tumor metastasis has been widely discussed but the specific mechanism has not been well-established. *L. johnsonii* has been identified as a potential beneficial bacterium that may improve memory impairment through the brain-gut axis[28] and regulate metabolic-related diseases[29]. Wu et al. have reported that *L. johnsonii* could alleviate colitis by inhibiting M1 macrophage polarization through modulation of the MAPK pathway[30]. Furthermore, oral administration of *L. johnsonii* has been found to enhance levels of tight junction proteins ZO-1 and occludin in colitis[31]. It has been observed that *L. johnsonii* acts as a repair agent for gut mucosal immunity and barrier in the gastrointestinal tract. In our study, we established an in vitro coculture system with *L. johnsonii* stimulation on IHH4 cells to investigate its effects on human PTC cells. Our findings indicated that *L. johnsonii* can suppress the proliferation and migration of PTC cells. Additionally, we conducted a xenograft tumor experiment in nude mice to confirm that *L. johnsonii* can inhibit the LNM of PTC in vivo. Activation of the Wnt/β-catenin pathway plays a crucial role in tumor growth and metastasis. Research indicates that *L. johnsonii* inhibits the progression of colorectal cancer by suppressing the β-catenin/c-MYC pathway[32]. Wnt/β-catenin pathway can regulate the

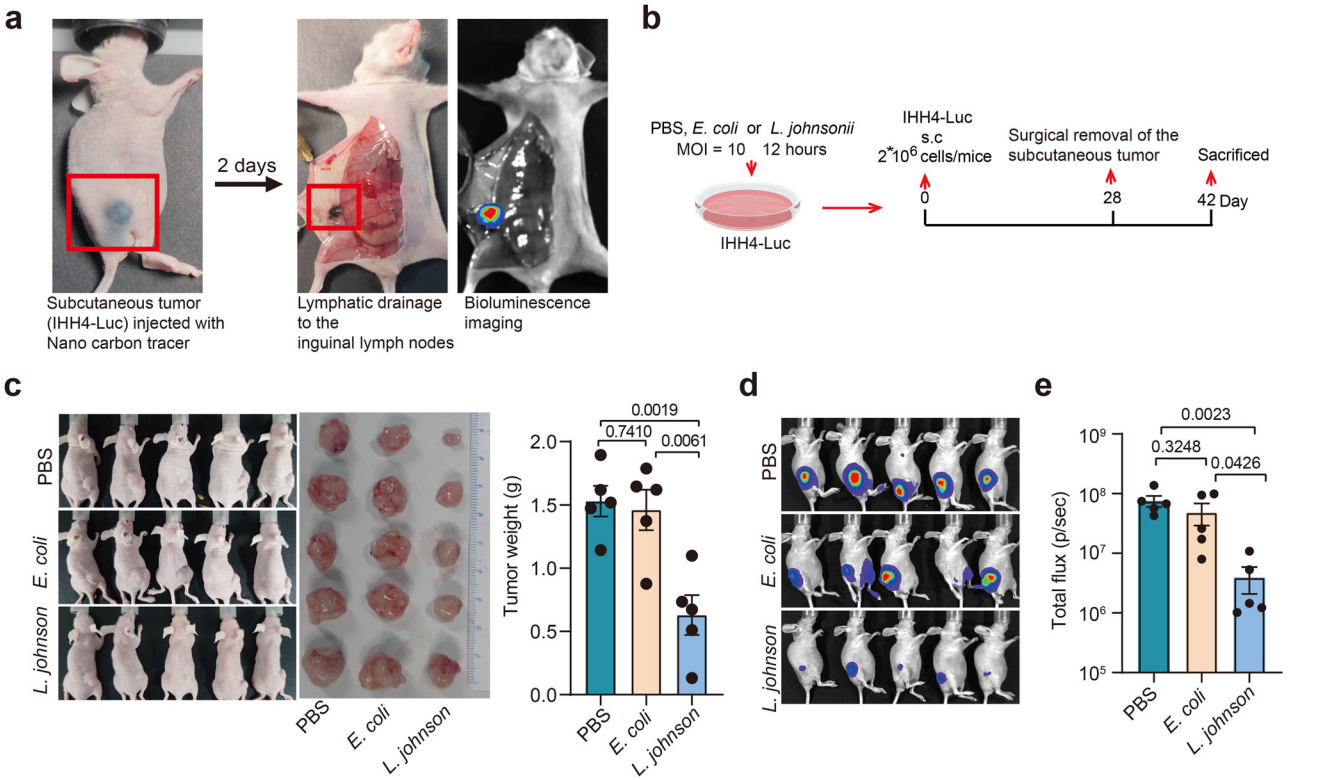

Fig. 5 | *L. johnsonii* suppressed tumor growth and LNM of PTC in vivo. a The metastatic lymph nodes were labeled by Luciferase and nano carbon tracer. **b** Schematic representation of protocol of PTC xenograft tumor experiment in nude mice (see details in Methods). **c** The in vivo tumor growth status of *L. johnsonii*, *E. coli* and PBS pretreated groups were demonstrated by photos. **d** Comparisons of tumor weight among the three groups. **e** Bioluminescence imaging was used to monitor LNM after removing subcutaneous tumor. **f** Comparisons of luciferase activity of metastatic lymph node among the three groups. $n = 5$ biologically independent samples for each group. Error bars indicate standard error of the mean.

transcription of c-MYC to promote tumor growth and facilitate tumor metastasis by regulating EMT-related genes. EMT was known to enhance invasiveness and metastatic potential in solid tumors[33]. We observed a significant inhibition of the EMT in PTC cells when co-cultured with *L. johnsonii*. Furthermore, our results showed that after co-cultured with *L. johnsonii*, there was a decrease in the expression of β-catenin, c-MYC, N-cadherin, and Vimentin, concomitant with a notable increase in E-cadherin levels in IHH4 and TPC1 cells. These findings mark the initial steps in understanding how *L. johnsonii* influences the LNM in PTC, providing a foundation for further investigation into its mechanisms.

The presence of bacterial communities in the tumor environment, which were also commonly found in the gut microbiome, indicated the potential occurrence of bacterial translocation from the gut to tumors in other locations[34]. To explore the potential clinical application of treating PTC, we conducted a gut colonization experiment to examine the effect of *L. johnsonii* on LNM in PTC. However, the absence of mouse PTC cell lines prevented the establishment of an allograft tumor model, thus presenting a methodological constraint in this study. Interestingly, our experiment involved xenograft tumors in nude mice coincidentally revealed that administering *L. johnsonii* through gavage significantly increased the presence of intratumoral *L. johnsonii* and inhibited the LNM of PTC. This finding was significant as previous studies have assumed that *Lactobacillus* colonization in the intestine exerts anti-tumor effects by promoting T-cell activation[20,35]. However, our results demonstrated that intestinal colonization of *L. johnsonii* could directly impact tumor cells and inhibit LNM of PTC even in the absence of T-cell involvement. Since the mechanisms of intratumoral bacteria influence tumor biology remain poorly understood, it has been hypothesized that bacteria may indirectly affect LNM of PTC by altering the local inflammation and immune microenvironment after migrating from the gut to the thyroid. However, our findings suggested that *L. johnsonii* may directly modulate the Wnt/β-catenin pathway in PTC cells, thereby inhibiting lymph node metastasis, a process that does not appear to involve inflammation or immune cells. Therefore, the oral consumption of *L. johnsonii* may hold potential as a treatment modality for PTC.

Inevitably, this study has a few limitations. While our sample size provided valuable insights into the involvement of intratumoral bacteria in PTC, the results must be validated by future study with larger sample size. Furthermore, the absence of a control group consisting of individuals with benign nodules may hinder the interpretation of the results. Comparing the microbial disparities in thyroid tissues between patients with benign nodules and those with PTC would further bolster the observations made in this study.

In conclusion, this study employed 16S rRNA gene sequencing alongside in vitro and in vivo experiments to elucidate the prevalence of *L. johnsonii* and substantiate its involvement and mechanisms in the LNM of PTC. Our results provided evidence that intratumoral *L. johnsonii* possesses the ability to impede tumor growth and metastasis in PTC, suggesting that oral administration of *L. johnsonii* could be a promising therapeutic approach for PTC.

Methods

Mice experiments

Mice experiments were carried out in accordance with the guidelines approved by the Institutional Animal Care and Use Committee (IACUC) of the First Affiliated Hospital of Nanchang University (CDYFY-IACUC-202308QR020). 5–6 week old female BABL/C nude mice were purchased from Guangzhou GemPharmatech Co., Ltd. (Guangzhou, China). Animals were housed in a specific pathogen-free condition and fed standard mouse chow. Manual randomization was used to allocate mice to the experiment groups. We have complied with all relevant ethical regulations for animal use.

IHH4-Luc cells were plated for 12 h followed by medium replacement with penicillin–streptomycin (P/S) free DMEM (10% FBS) and then

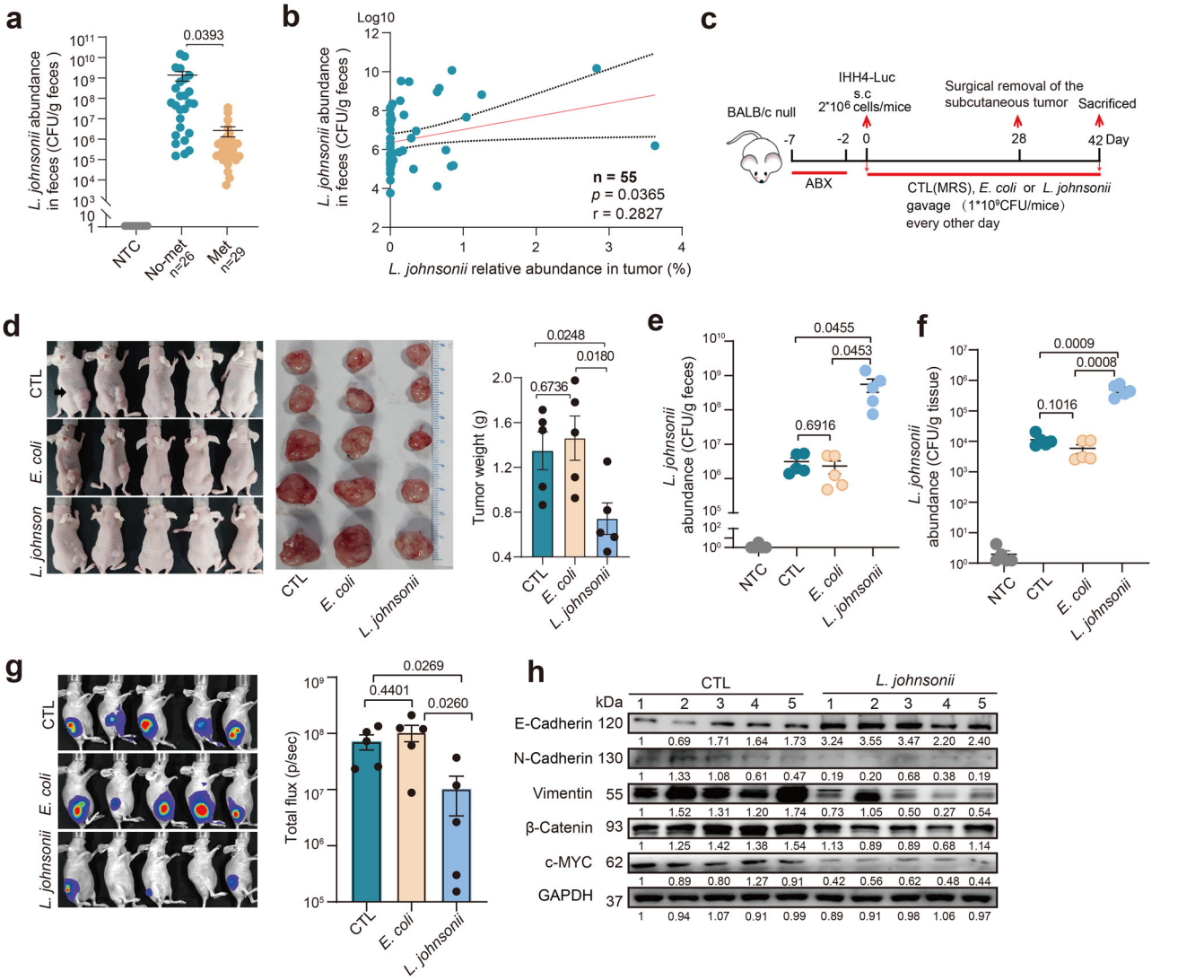

Fig. 6 | Gut colonization of *L. johnsonii* inhibited PTC metastatic progression. **a** qPCR analysis of *L. johnsonii* abundance in the feces of PTC patients. **b** The correlation analysis of *L. johnsonii* abundance between tumors and feces of PTC patients. **c** Schematic representation of bacterium intestinal colonization experimental protocol in nude mice (see details in Methods). **d** Photographs demonstrated xenograft mice and their surgically excised tumors from the *L. johnsonii*, *E. coli*, and MRS gavaged groups, with a comparison of tumor weights among the three groups. **e**, **f** Comparisons of the abundance of *L. johnsonii* in mice fecal (**e**) and xenograft tumors (**f**) between the three groups. **g** Bioluminescence imaging and luciferase fluorescence of metastatic lymph node in the three groups. **h** Western blot analysis for Wnt/β-catenin pathway expression in xenograft tumors with or without gut colonization of *L. johnsonii*. $n = 5$ biologically independent samples for each group. Error bars indicate standard error of the mean.

co-cultured with bacteria (*L. johnsonii* or *E. coli*) at a multiplicity of infection (MOI) of 10:1 for another 12 h under anaerobic conditions at 37 °C. Cells were washed with sterile 1×PBS three times and cultured in DMEM (1% P/S, 10% FBS) medium for 8 h to kill any remaining bacteria. Finally, the cells were collected and injected subcutaneously into BABL/C nude mice (2×10^6 cells/mice) (*L. johnsonii*, *E. coli* and PBS pretreated groups; $n = 5$ in each group; total 15 mice). On day 28, the subcutaneous tumor was surgically resected and the wound was sutured. The metastasis of inguinal lymph nodes was evaluated on day 42 by measuring luciferase fluorescence via In Vivo Imaging System (AniView). Each mouse received an intraperitoneal (i.p.) injection of 200 μL luciferin (15 mg/mL; Meilunbio, #MB1834-2) and the luciferase signal was captured after 10 min. Mice were then sacrificed. For bacterial colonization in gut, mice were given an antibiotic cocktail containing vancomycin (100 mg/L), metronidazole (200 mg/L), ampicillin (200 mg/L) and neomycin (200 mg/L) in the drinking water for 5 days. After 48 h washout period, mice were gavaged with bacteria (1×10^9 CFU/mouse) or MRS every other day until the end of the experiment (*L. johnsonii*, *E. coli* and MRS gavaged groups; $n = 5$ in each group; total 15 mice). IHH4-Luc cells were injected subcutaneously into BABL/C nude mice on day 0, and the subcutaneous tumor was surgically resected and the wound was sutured on day 28. On day 42, the progression of the metastatic lymph nodes was evaluated as described above. The treatment and measurement order were counterbalanced across animals, so that each treatment condition was applied at different times, ensuring no systematic order bias. Tumor size was the primary outcome measure.

Human specimens collection

The fecal samples of PTC patients and PTC paired tumor and normal specimens were collected from the First Affiliated Hospital of Nanchang University. PTC patients with LNM (Metastasis group) or without LNM (Non-metastasis group) were recruited in our study. The exclusion criteria included the use of antibiotics within one month, oral and neck infectious diseases, and other concurrent severe organic diseases. Finally, 55 patients were recruited in our study (Metastatic group, $n = 29$; Non-metastasis group, $n = 26$). Postoperative pathological results showing positive lymph nodes were defined as the presence of LNM. The protocol of human sample

usage and the informed consent were approved by the Ethical Review Board of the First Affiliated Hospital of Nanchang University [(2023)CDY-FYYLK(07-008)]. All patients signed informed consent forms. All ethical regulations relevant to human research participants were followed.

Cell lines and bacterial strains culture

IHH4, TPC1 and IHH4-Luciferase (Luc) cell lines were cultured in DMEM medium (Gibco, #DMEM) supplemented with 10% fetal bovine serum (HyClone, #SV30160) and 1% penicillin–streptomycin (Gibco, #15140122). The *L. johnsonii* strains were cultured on Man Rogosa Sharpe (MRS, Oxoid, #CM1175B) plates under anaerobic conditions at 37 °C for 48 h. *E. coli* was cultured on Brain Heart Infusion (BHI, BD, #237500) plates under aerobic conditions at 37 °C. All cell lines were purchased from Procell Life Science & Technology Co., Ltd. (IHH4: CL-0803, TPC1: CL-0643; Wuhan, China).

qPCR quantification

The colonization of *L. johnsonii* in feces and its translocation in tumor were assessed by qPCR, as previously described[25]. *L. johnsonii* DNA was used to plot a standard curve to calculate *L. johnsonii* DNA concentration in the sample and the steriled enzyme-free water served as negative control (NTC) for the reactions[25,36]. Tumor and feces were weighted followed by total DNA extraction using the DNeasy Blood & Tissue Kit (for tumor, QIAGEN, #69504) or HiPure Stool DNA Kit (for feces, Magen, #D3141-02).

For qPCR quantification, briefly, 10 uL reaction mix containing 3 uL steriled enzyme-free water (Solarbio, #R1600-500ml), 5 uL TB Green® Premix Ex Taq™ (TAKARA, #RR420A), 0.5 uL forward primer (5′-TCGAGCGAGCTTGCCTAGATGA-3′), 0.5 uL reverse primer (5′-TCCGGACAACGCTTGCCACC-3′), and 1 uL sample DNA, was loaded on the Applied Biosystems 7500 Real-time PCR system. Raw cycle threshold (Ct) values were normalized according to a bacterial standard curve produced with *L. johnsonii* DNA.

Fluorescence in situ hybridization (FISH)

Paraffin sections were deparaffinized and then incubated in lysozyme solution (10 mg/mL) at 37 °C. *L. johnsonii* probes were Cy3-conjugated specific probe (5'-AGCTTCAATCTTCAGGAT-3') and were manufactured by Wuhan servicebio Technology. Slides were incubated with probe diluted in prewarmed hybridization buffer overnight at 40 °C in a humid chamber. Slides were subsequently washed three times with prewarmed (37 °C) washing buffer and Tris buffer, respectively. Tissues were stained by DAPI, and fluorescent signal capture using a confocal microscope (NIKON ECLIPSE CI, Japan). The fluorescence intensity of all the samples was evaluated using the ImageJ Fiji, and statistical analysis was performed.

CCK8 assay

IHH4 and TPC1 cells were stimulated by bacteria as described above. Then cell growth was assessed using the CCK8 assay. Briefly, IHH4 and TPC1 cells were seeded in 96-well plates (2×10^3 cells/well). The culture medium was removed the next day and 100 uL fresh medium containing 10 μL CCK8 solution were added to each well. After 1 h incubation, the absorbance was measured at 450 nm.

Migration and invasion assays

Tumor cells invasion and migration assays were carried out in Transwell chambers (Corning, #3422) with or without Matrigel® Basement Membrane Matrix (Corning, #356234). 200 μL cells in DMEM (FBS-free, 1% P/S) were seeded in the upper chamber (2×10^5 cells /well), with the bottom chamber filled with 600 μL DMEM (10% FBS, 1% P/S). After 24 h, cells were fixed with 4% paraformaldehyde for 15 min and stained with 0.2% crystal violet for 30 min. Images of invaded or migrated cells were captured from five random fields per condition with a microscopy. The bound crystal violet was eluted by adding 33% acetic acid into each insert and shaking for 10 min. The eluent from the lower chamber was transferred to a 96-well clear microplate, and the absorbance value (optical density, OD) at 570 nm was measured using Thermo Scientific Microplate Reader.

Western blot

Western blot was performed as previously described[37]. Tumor tissues and cell pellets were lysed using RIPA buffer (Beyotime, #P0013B) and protein concentration was quantified using BCA Protein Assay Kit (Thermofisher, #23227). GAPDH was used as an endogenous control. The following antibodies were used: anti-E-Cadherin (CST, #3195 T, 1:1000 dilution), anti-Vimentin (CST, #5741 T, 1:1000 dilution), GAPDH (CST, #2118 T, 1:1000 dilution), anti-N-Cadherin (CST, #13116 T, 1:1000 dilution), anti-β-catenin (CST, #8480 T, 1:1000 dilution), anti-c-MYC (CST, #5605 T, 1:1000 dilution).

β-catenin gene silencing

Lentiviruses were generated by co-transfecting HEK293T cells with packaging plasmids (psPAX2 and pMD2.G) using PEI MAX 40 K (Polyscience, Illinois, USA), and viral supernatants were collected after 48 h. Then, the virus-containing medium supernatants were used to infect IHH4 and TPC1 tumor cells using polybrene (1 μg/ml) methodology. Puromycin-resistant IHH4 cells (Puromycin, 1.5 μg/ml) and TPC1 cells (Puromycin, 2 μg/ml) were selected for the subsequent experiment. All shRNA sequences are listed as follows: shCTL: TTCTCCGAACGTGTCACGT, shβ-catenin#1: GCACAAGAATGGATCACAAGA, shβ-catenin#2: GCTGGTATCTCAGAAAGTGCC.

Bacteria culture and identification

Isolation of anaerobic or aerobic bacteria was performed as previously described. 100–200 mg tumor tissues were cut into pieces and homogenized in 1 mL ice-cold BHI under sterile conditions. 1×PBS was used as NTC and went through the same workflow to evaluate the environmental contaminants. For aerobic culture, 200 uL sample homogenate was plated on BHI plates at 37 °C aerobically with 5% CO_2.

For anaerobic culture, 200 uL sample homogenate was transferred to 5 mL BHI medium and cultured under anaerobic conditions for 2 days for bacterial enrichment, then 20 uL culture medium were plated on brucella broth agar plates (Bruce, BD, #211088) supplemented with 5% sheep citrated blood. The plates were incubated at 37 °C for 5 days in anaerobic conditions.

For identification of bacteria strain, colonies were picked and streaked in designated plate and condition for 1–3 days to get single colony. The single colony was picked to grow in plates and run colony PCR subsequently. Briefly, the 20 uL reaction mix contained 1 uL bacteria DNA, 8 uL steriled enzyme-free water (Solarbio, #R1600–500 ml), 10 uL 2× Taq plus MasterMix II (Dye plus) (Vazyme, #P213-03) and 0.5 uL forward primer (27 F: 5'-AGAGTTTGATCCTGGCTCAG-3'), 0.5 uL reverse primer (1492 R: 5'-GGTTACCTTGTTACGACTT-3'). The reaction was programmed according to the reagent instructions. The PCR product was sent out for sequencing and the sequencing results were aligned to the 16S rRNA sequences database in the NCBI BLAST site.

High throughput 16S rRNA amplicon sequencing and analysis

Genomic DNA was extracted using FastDNA Spin Kit for Soil (MP Biomedicals). In brief, barcoded amplicons from the V3-V4 region were generated using PCR. In the first step, 10 ng genomic DNA was used as template for the first PCR with a total volume of 20 μL using the 338 F (5'-ACTCCTACGGGAGGCAGCAG-3') and 806 R (5'-GGACTACHVGGGTWTCTAAT-3') primers appended with Illumina adaptor sequences. Subsequently, PCR products were purified, checked on a Fragment analyzer and quantified, followed by equimolar multiplexing, and sequencing on an Illumina MiSeq PE300 platform (2×300 bp). Quantitative Insights into Microbial Ecology 2 (QIIME2) software was used for microbial analyses. Reads were imported, quality filtered and demultiplexed with the q2-data2 plugin. The sequences were classified using Greengenes (version 13.8) as a reference 16S rRNA gene database. Principal Coordinate Analysis (PCoA), Linear discriminant analysis effect size (LEfSe) and Significant Species were performed using R (v4.1.1). 16S rDNA data are available from the Genome Sequence Archive (GSA, https://ngdc.cncb.ac.cn/gsa) under accession number PRJCA022672.

Statistics and reproducibility

Statistical analysis and data visualization carried out in this study was performed by GraphPad Prism 8. The data were presented as means ± SEM. Differences between two groups were compared using unpaired Student's t-tests. Comparisons among three or more groups were performed by one-way ANOVA test combined with Tukey's multiple comparison test. Differences in clinical characteristics of patients were determined using Pearson's chi-squared test or Fisher's exact test, as appropriate. All p values were two-tailed, and differences with a p value less than 0.05 were considered significant.

Reporting summary

Further information on research design is available in the Nature Portfolio Reporting Summary linked to this article.

Data availability

Source data for the graphs are provided as Supplementary Data 1. The uncropped full scans of western blots are provided as Supplementary Fig. 2. 16S rDNA data are available from the Genome Sequence Archive (GSA, https://ngdc.cncb.ac.cn/gsa) under accession number PRJCA022672. All materials and data are available upon request from the corresponding authors.

Code availability

This paper did not produce the original code.

Received: 30 June 2024; Accepted: 28 February 2025;
Published online: 12 March 2025

References

1. Sung, H. et al. Global cancer statistics 2020: GLOBOCAN estimates of incidence and mortality worldwide for 36 cancers in 185 countries. *CA Cancer. J. Clin.* **71**, 209–249 (2021).
2. Chen, D. W., Lang, B., Mcleod, D., Newbold, K. & Haymart, M. R. Thyroid cancer. *Lancet* **401**, 1531–1544 (2023).
3. Koo, B. S., Choi, E. C., Park, Y. H., Kim, E. H. & Lim, Y. C. Occult contralateral central lymph node metastases in papillary thyroid carcinoma with unilateral lymph node metastasis in the lateral neck. *J. Am. Coll. Surg.* **210**, 895–900 (2010).
4. Pinheiro, R. A. et al. Incidental node metastasis as an independent factor of worse disease-free survival in patients with papillary thyroid carcinoma. *Cancers* **15**, 943 (2023).
5. Roy, S. & Trinchieri, G. Microbiota: a key orchestrator of cancer therapy. *Nat. Rev. Cancer* **17**, 271–285 (2017).
6. Parhi, L. et al. Breast cancer colonization by Fusobacterium nucleatum accelerates tumor growth and metastatic progression. *Nat. Commun.* **11**, 3259 (2020).
7. Bertocchi, A. et al. Gut vascular barrier impairment leads to intestinal bacteria dissemination and colorectal cancer metastasis to liver. *Cancer Cell* **39**, 708–724 (2021).
8. Routy, B. et al. Gut microbiome influences efficacy of PD-1-based immunotherapy against epithelial tumors. *Science* **359**, 91–97 (2018).
9. Feng, J. et al. Alterations in the gut microbiota and metabolite profiles of thyroid carcinoma patients. *Int. J. Cancer.* **144**, 2728–2745 (2019).
10. Zheng, L. et al. Gut microbiota is associated with response to 131I therapy in patients with papillary thyroid carcinoma. *Eur. J. Nucl. Med. Mol. Imaging* **50**, 1453–1465 (2023).
11. Helmink, B. A., Khan, M., Hermann, A., Gopalakrishnan, V. & Wargo, J. A. The microbiome, cancer, and cancer therapy. *Nat. Med.* **25**, 377–388 (2019).
12. Yuan, L. et al. Tumor microbiome diversity influences papillary thyroid cancer invasion. *Commun. Biol.* **5**, 864 (2022).
13. Dai, D. et al. Alterations of thyroid microbiota across different thyroid microhabitats in patients with thyroid carcinoma. *J. Transl. Med.* **19**, 488 (2021).
14. Su, X., Zhao, Y., Li, Y., Ma, S. & Wang, Z. Gut dysbiosis is associated with primary hypothyroidism with interaction on gut-thyroid axis. *Clin. Sci. (Lond).* **134**, 1521–1535 (2020).
15. Zhou, L. et al. Gut microbe analysis between hyperthyroid and healthy individuals. *Curr. Microbiol.* **69**, 675–680 (2014).
16. Cayres, L. et al. Detection of alterations in the gut microbiota and intestinal permeability in patients with Hashimoto thyroiditis. *Front. Immunol.* **12**, 579140 (2021).
17. Alfano, M. et al. The interplay of extracellular matrix and microbiome in urothelial bladder cancer. *Nat. Rev. Urol.* **13**, 77–90 (2016).
18. Liu, H. X. et al. Difference of lower airway microbiome in bilateral protected specimen brush between lung cancer patients with unilateral lobar masses and control subjects. *Int. J. Cancer.* **142**, 769–778 (2018).
19. Xie, Y. et al. Microbiota in tumors: from understanding to application. *Adv. Sci.* **9**, e2200470 (2022).
20. Bender, M. J. et al. Dietary tryptophan metabolite released by intratumoral Lactobacillus reuteri facilitates immune checkpoint inhibitor treatment. *Cell* **186**, 1846–1862 (2023).
21. Kohi, S. et al. Alterations in the duodenal fluid microbiome of patients with pancreatic cancer. *Clin. Gastroenterol. Hepatol.* **20**, e196–e227 (2022).
22. Qu, D. et al. Intratumoral microbiome of human primary liver cancer. *Hepatol. Commun.* **6**, 1741–1752 (2022).
23. Riquelme, E. et al. Tumor microbiome diversity and composition influence pancreatic cancer outcomes. *Cell* **178**, 795–806 (2019).
24. Knippel, R. J., Drewes, J. L. & Sears, C. L. The cancer microbiome: recent highlights and knowledge gaps. *Cancer Discov.* **11**, 2378–2395 (2021).
25. Fu, A. et al. Tumor-resident intracellular microbiota promotes metastatic colonization in breast cancer. *Cell* **185**, 1356–1372 (2022).
26. Liu, J. & Zhang, Y. Intratumor microbiome in cancer progression: current developments, challenges and future trends. *Biomark. Res.* **10**, 37 (2022).
27. Laniewski, P. et al. Linking cervicovaginal immune signatures, HPV and microbiota composition in cervical carcinogenesis in non-Hispanic and Hispanic women. *Sci. Rep.* **8**, 7593 (2018).
28. Wang, H. et al. Lactobacillus johnsonii BS15 prevents psychological stress-induced memory dysfunction in mice by modulating the gut-brain axis. *Front. Microbiol.* **11**, 1941 (2020).
29. Yang, G., Hong, E., Oh, S. & Kim, E. Non-viable Lactobacillus johnsonii JNU3402 protects against diet-induced obesity. *Foods* **9**, 1494 (2020).
30. Wu, Z. et al. Propionic acid driven by the Lactobacillus johnsonii culture supernatant alleviates colitis by inhibiting M1 macrophage polarization by modulating the MAPK pathway in mice. *J. Agric. Food. Chem.* **71**, 14951–14966 (2023).
31. Yuan, L. et al. Lactobacillus johnsonii N5 from heat stress-resistant pigs improves gut mucosal immunity and barrier in dextran sodium sulfate-induced colitis. *Anim. Nutr.* **15**, 210–224 (2023).
32. Cao, Q. et al. Chronic stress dampens lactobacillus johnsonii-mediated tumor suppression to enhance colorectal cancer progression. *Cancer Res.* **84**, 771–784 (2024).
33. Heerboth, S. et al. EMT and tumor metastasis. *Clin. Transl. Med.* **4**, 6 (2015).
34. Lloyd-Price, J. et al. Strains, functions and dynamics in the expanded Human Microbiome Project. *Nature* **550**, 61–66 (2017).
35. Fong, W. et al. Lactobacillus gallinarum-derived metabolites boost anti-PD1 efficacy in colorectal cancer by inhibiting regulatory T cells through modulating IDO1/Kyn/AHR axis. *Gut* **72**, 2272–2285 (2023).
36. Ibekwe, A. M., Watt, P. M., Grieve, C. M., Sharma, V. K. & Lyons, S. R. Multiplex fluorogenic real-time PCR for detection and quantification of Escherichia coli O157:H7 in dairy wastewater wetlands. *Appl. Environ. Microbiol.* **68**, 4853–4862 (2002).

37. Xie, M. et al. Adiponectin alleviates intestinal fibrosis by enhancing AMP-activated protein kinase phosphorylation. *Dig. Dis. Sci.* **67**, 2232–2243 (2022).

Acknowledgements
This work was supported by the Science and Technology Plan of Jiangxi Provincial Health Commission (202130202) and the Jiangxi Provincial Natural Science Foundation (20224BAB216022, 20232BAB206020).

Author contributions
X.M. and L.F.: Study conception and design. X.M. and M.X.: Study supervision and funding acquisition. M.X., T.Y., Q.L. and Z.N.: Sample processing, data curation, data analysis, data interpretation and manuscript writing. X.M., Q.L. and T.Y.: Patient recruitment and sample collection. M.X. and L.F.: Manuscript editing and review. All authors reviewed the results and approved the final version of the manuscript.

Competing interests
The authors declare no competing interests.

Additional information
Supplementary information The online version contains supplementary material available at https://doi.org/10.1038/s42003-025-07856-9.

Correspondence and requests for materials should be addressed to Lili Feng or Xiang Min.

Peer review information *Communications Biology* thanks the anonymous reviewers for their contribution to the peer review of this work. Primary Handling Editors: Kaliya Georgieva. A peer review file is available.